PROCEEDINGS OF SCIENCE

GRB 221009A: The brightest burst of all time as seen by Fermi-LAT

E. Bissaldi,[1,2,*] **P. Bruel,**[3] **N. Di Lalla,**[4] **N. Omodei**[4] **and R. Pillera**[1,2]
on behalf of the Fermi-LAT Collaboration

[1] *Dipartimento Interateneo di Fisica dell'Università e del Politecnico di Bari, 70125 Bari, Italy*
[2] *INFN Sezione di Bari, 70125 Bari, Italy*
[3] *Laboratoire Leprince-Ringuet, CNRS/IN2P3, École polytechnique, Institut Polytechnique de Paris, F-91120 Palaiseau, France*
[4] *Department of Physics and Kavli Institute for Particle Astrophysics and Cosmology, Stanford University, Stanford, CA 94305, USA*

E-mail: elisabetta.bissaldi@ba.infn.it

On October 9, 2022, the brightest GRB ever detected, also called the "Brightest Of All Time" (or BOAT), was detected by the Fermi Large Area Telescope (LAT), providing an unprecedented rich dataset that will likely help to understand the emission mechanisms underlying this class of extra-galactic objects. Some of the unique features of GRB221009A include: 1) high-energy (up to 100 MeV) emission observed during the first emission episode (precursor) at the GBM trigger time T_0; 2) Several GeV events, including a 100 GeV photon, observed during the brightest emission episode; and 3) a very long-lived high-energy extended emission phase covering tens of kiloseconds, with a peculiar 400 GeV photon observed at almost 10 hours after T_0. Here we review all these observations, focusing especially on the efforts that the Fermi LAT collaboration made in order to understand and recover part of the data affected by the extremely high soft gamma-ray noise during the brightest emission episode at T_0 + 200 s.

38th International Cosmic Ray Conference (ICRC2023)
26 July - 3 August, 2023
Nagoya, Japan

*Speaker

PoS(ICRC2023)847

1. Introduction

GRB 221009A represents an exceptional and quite unique gamma-ray burst, which broke many previous records, not only at high energies, but over many energy bands, quickly deserving the title of the “Brightest Of All Time", or the “B.O.A.T." GRB. This event was so strong and long-lived that it was detected by dozens of space and ground-based observatories, resulting in more than 120 rapid observation reports and communications of the Gamma-Ray Coordinate Network (GCN) and of The Astronomer’s Telegram (ATEL) since the very beginning of observations, and over 50 publications, including discussions about its X-ray, radio and optical observations, as well as several follow-up campaigns carried out by e.g. VHE telescopes and neutrino observatories. The burst’s spectroscopic redshift was found to be $z = 0.1505$ [1].

Here we report Fermi-LAT observations of this remarkable event, which was first discovered by the Fermi Gamma-Ray Burst Monitor (GBM) on 2022 October 9 at 13:16:59.988 UT [2]. We refer to this time as T_0 of the burst and note that this preceded by about an hour the *Swift* Burst Alert Telescope (BAT) detection circular, tentatively classifying the trigger as a new source called *Swift* $J1913.1+1946$ [3] with possible Galactic origin, given its proximity (~ 4 deg) to the Galactic plane.

Due to its extreme brightness, GRB 220910A caused major saturation effects in both the LAT and the GBM detectors during the main emission episode at $T_0 + 200$ s. Therefore, we first present prescription on how to treat LAT data during the so-called Bad Time Interval (BTI). Then we discuss the analysis of the GRB emission phases, focusing on the triggering pulse, the prompt emission and the temporally extended emission and their properties. We briefly discuss the highest-energy photons detected by LAT and we conclude by comparing GRB 221009A with the other LAT detected GRBs. More details about the analysis will be available in a forthcoming publication.

2. Analysis and fitting procedures

During the prompt emission, the peculiar brightness of GRB 221009A caused a large X-ray and soft gamma-ray ($E < 10$ MeV) flux that produced very high levels of noise in the LAT subsystems (Tracker, Calorimeter and Anti Coincidence Detector, ACD). Since the instrument and the event reconstruction were not designed to deal with such conditions, we had to carefully select the time intervals during which it is possible to use standard analysis methods, either `fermitools` or the LAT Low Energy Event technique (LLE).

LAT event reconstruction can be affected by so-called "ghost" signals, i.e. remnants of signals due to particle passing through the instrument a few μs before a trigger is issued. Thanks to the Pass 8 effort [4] to improve the event reconstruction, this effect was mitigated. In fact, it is possible to measure this noise with events that are recorded independently of the activity in the instrument thanks to a 2 Hz `PERIODIC` trigger (PT). Almost all of the ghost signals correspond to only one out-of-time particle.

We focused our data inspection on the brightest part of the GRB emission, in a time interval from $T_0 + 200$ s to $T_0 + 300$ s, and plotted the logarithm of the number of fired strips in the tracker as a function of time, as can be seen in Fig 1. Fired strips for the events with at least one track that passed the main gamma-ray trigger and on-board filter are shown as black points, fired strips

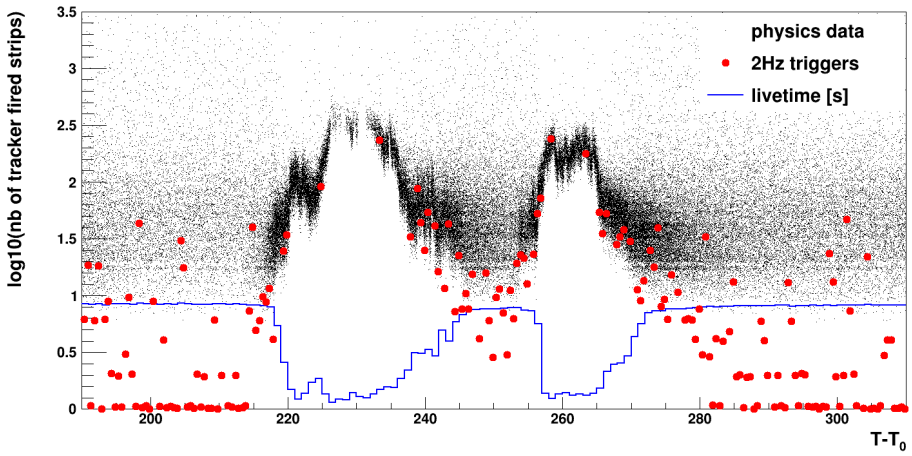

Figure 1: Number of tracker fired strips in the events with at least one track that pass the gamma-ray main trigger and on-board filter as a function of time since the GBM trigger (black dots). The red dots correspond to the events triggered with a 2 Hz cadence to monitor the noise in the instrument. The blue histogram shows the livetime recorded in the 1 second spacecraft file.

for the PT events are shown as red points. Prior $T_0 + 217$ s and after $T_0 + 280$ s the data taking is characterized by normal operational conditions, with just a few PT events with more than 10 strips corresponding to remnants of out-of-time cosmic rays.

This behaviour changes completely during the burst's main emission, characterized by two consequent peaks affected by data issues. It can be seen that the number of fired strips in PT events is most of the time greater than 10 and can even exceed 100. Unfortunately, due to very high deadtime, only a few PT events are recorded during the brightest parts of the burst. The bottom edge of the main-trigger event distribution can be used to estimate the noise in the tracker as a function of time and note that it exceeds 100 during both emission peaks. Studying how the noise impacted the event reconstruction and selection over the whole time window of Fig 1, we conclude that (1) data in the two time intervals $T_0 + 219$ s $- T_0 + 244$ s and $T_0 + 255$ s $- T_0 + 270$ cannot be analysed with any standard procedure; and (2) data in the three time intervals $T_0 + 217$ s $- T_0 + 219$ s, $T_0 + 244$ s $- T_0 + 255$ s, and $T_0 + 270 - T_0 + 280$ can be analysed with the `TRANSIENT_010E` event class but only above 125 MeV and taking into account an average inefficiency of 0.75 ± 0.25.

The fitting procedures adopted in the temporal and spectral analysis of Fermi GBM and Fermi LAT data are part of `ThreeML` [5], a python-based software package for parameter inference using the maximum likelihood formalism (with Bayesian posterior sampling supported as well). Depending on the instrumental condition, and on the viewing angle of burst with respect to the various detectors, we combined different datasets and used different plugins. In all our analysis we used the best known localization of R.A. = 288°.264587 Dec. = 19°.773397 reported by [6].

The broad-band lightcurve of GRB 221009A is shown in Figure 2. The top three rows show the low-energy GBM NaI (n4 and n7) and BGO (b1) detector lightcurves (green histograms), followed by the LLE (blue histogram) and LAT (red histogram) light curves. The bottom rows displays LAT `TRANSIENT_010E` events with energy greater than 100 MeV. Panels on the left represent a

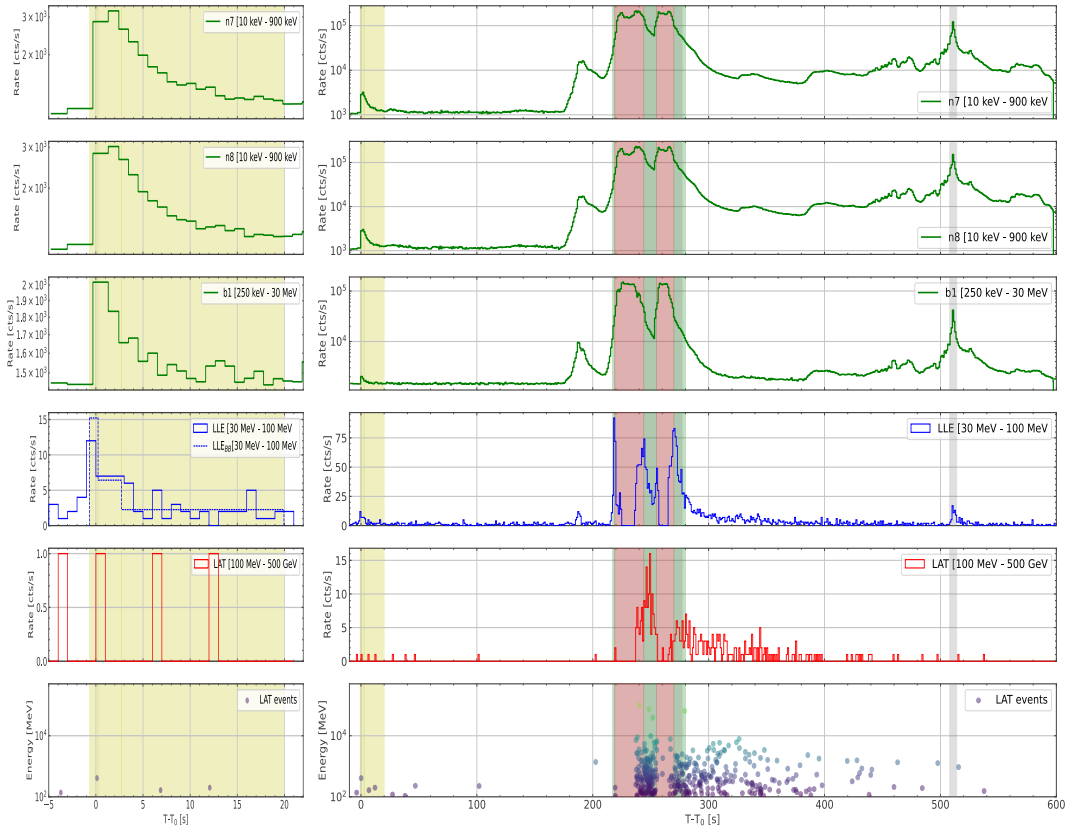

Figure 2: Left panels: light curves of the bright triggering pulse; Right panels: light curves of the entire 600 seconds interval after T_0 showing the main emission across the broad gamma-ray band, including the shaded regions indicating the LAT BTIs (green areas correspond to intervals when LAT data can be used with the prescription described in the text, red areas to intervals which are not usable, grey areas are the GBM BTIs [7]. Yellow is the interval selected for joint spectral analysis of the triggering pulse. The GBM light curves (first three panels) are not corrected for pulse pile-up. [7].

zoom-in on the first burst emission episode, which we refer to as "the triggering pulse", from T_0 to $T_0 + 20$ s (yellow shaded area). We refer to the subsequent emission as "the prompt emission", lasting approximately 10 minutes.

3. Main analysis results and Discussion

The spectral analysis of **the triggering pulse** was performed in the time interval $T_0 - 0.69$ s to $T_0 + 19.95$ s by including (1) GBM TTE data in their nominal energy range from detectors n4, n7 and b1, which have the best viewing angles with respect to the source; (2) LLE data from 30 MeV to 100 MeV; and (3) LAT `TRANSIENT_010E` (> 100 MeV) data. We tested different phenomenological spectral models (simple power law (PL), Band, Comptonized (COMP) and double smoothly broken power law (2SBPL), see [8]) and investigated the presence of extra PL components for the COMP, Band and 2SBPL models. By comparing different models by means of the Bayesian Information Criterion (BIC), we conclude that COMP is the preferred model to describe the triggering pulse both when performing a time-integrated and a time-resolved spectral analysis. The peak energy

(E_{peak}) reaches a value of ∼15 MeV right at the peak onset, accompanied by a hard spectral index, rapidly decreasing to below 1 MeV after $T_0 + 7$ s, where the emission becomes overall softer. We also checked the quiescent period from $T_0 + 19.95$ s to $T_0 + 175$ s, but no significant detection of the GRB could be found in either standard LAT nor LLE data, leading to the derivation of flux upper limits.

During **the prompt phase** we jointly analysed GBM, LLE and LAT data, separately investigating the intervals before (from $T_0 + 175$ s to $T_0 + 219$ s) and after (from $T_0 + 280$ s to $T_0 + 435$ s) the BTIs. At later times, the GRB position rapidly moves out ot the LAT Field of View (FoV) – at $T_0 + 435$ s the angle is already $\sim 80°$. Even if the pulse at $T_0 + 510$ s is clearly visible in the LLE event selection (see Figure 1), at these large incident angles the instrument response functions are not well modeled, so we did not perform any spectral analysis.

In each of these time windows, we divided and analyzed the data in several intervals and in two energy bands (10–100 MeV and 100 MeV–100 GeV). We found that (1) before the BTIs, the LAT flux increased rapidly, following the behaviour at lower energies; (2) after the BTIs, the flux photon index remained quite hard, when compared to other LAT GRBs, peaking at $\Gamma = -1.6 \pm 0.1$ between $T_0 + 325$ s to $T_0 + 355$ s. Consequently, the >100 MeV flux remained high during this interval as opposed to the steady decay observed at lower energies (10–100 MeV). Using template fitting, we also estimated the photon index ($\Gamma = -1.8$) and the value of the energy flux ($\sim 10^{-4}$ erg cm^{-2} s^{-1} for 0.1–100 GeV) during the time interval $T_0 + 244$ s to $T_0 + 255$ s (the "bridge" between the two BTIs), and we note that the latter provides only a rough lower limit. A table listing detailed results, including best spectral models used, data intervals and data types, energy flux and photon index values, will be published in the upcoming publication.

While calculating the probability for each event to be associated with the GRB, following the prescriptions in [9], we found that during the BTIs there are four events with reconstructed energy greater than 10 GeV and with an association probability of $\sim$ 100%. The highest of these events carries an energy of 99 GeV, representing the highest photon energy recorded so far by the LAT during the prompt emission. Moreover, the energy (> 10 GeV) of these events is not affected by the extra noise in the calorimeter, whose average energy deposition per event was < 100 MeV. On the other hand, due to the higher deadtime suffered by the LAT during the BTIs, we cannot exclude that some other high-energy events entered the detector but did not trigger it. Therefore, the number of events above 10 GeV should only be treated as a lower limit.

For **the late time emission**, we analysed data after GRB 221009A re-entered the LAT FoV, starting at $T_0 + 3918$ s. We first computed the exposure as a function of time. Considering that the typical decay time for gamma-ray emission goes as T^{-1}, we multiplied the exposure by $(\mathrm{T} - \mathrm{T}_0)^{-1}$, providing us with a proxy for defining a temporal binning with an approximately constant number of expected events. Until $T_0 + 40$ ks we performed un-binned likelihood analysis, while between $T_0 + 40$ ks and $T_0 + 10^6$ s, given the longer exposures, we switched to binned likelihood analysis. During this emission, LAT detected three events with energy above 10 GeV. one of those having an energy of 400 GeV [10] arriving at $T_0 + 33$ ks.

The nature of the late-time LAT emission from $\sim T_0 + 4 \times 10^3$ s to $\sim T_0 + 3 \times 10^5$ s is similar to the high-energy extended emission detected in other LAT GRBs and is thought to be due to synchrotron emission from an external forward shock. The temporal decay of the flux during this time is $F_\nu \propto T^{-1.2\pm0.1}$, or $T^{-1.4\pm0.1}$, depending on the model, which is in between the $F_\nu \propto t^{-1}$ and

$F_\nu \propto t^{-10/7}$ flux decay expected for an adiabatic blastwave and a radiative blastwave, respectively. However, an adiabatic blastwave is favored from previous LAT detections [9]. The onset time of this afterglow is rather uncertain, partly because of a lack of LAT data prior to $\sim T_0 + 4 \times 10^3$ s (when the burst was outside the LAT FoV) and partly because of the very bright pulse detected by LAT peaking at $\sim T_0 + 240$ s. Because of the very steep decay of the flux at $\gtrsim T_0 + 240$ s, the LAT high–energy detection before $\sim T_0 + 300$ s is very unlikely originated from the afterglow forward shock emission, but it rather represents prompt emission from internal shocks. A second pulse is detected also around $\sim T_0 + 330$ s. We derived Lorentz factors by identifying the peak time with the deceleration time of the afterglow, and by using the kinetic energy E_K from [7]. Fitting the LAT lightcurve with a two component model, we obtained values of $\Gamma \sim 200 - 240$ for a wind case scenario, while we got $\Gamma \sim 360 - 480$ for a constant density Interstellar Medium (ISM) in the case of a fit with three components. We note that these values are lower limits on the outflow Lorentz factor, which can be significantly higher for a relativistic reverse shock (i.e. a "thick shell", which is likely the case for this GRB). We also provided an estimate of the burst energetics, finding a fluence ranging from 4.3 to 6.6×10^{-3} erg cm^{-2} in the 0.1–100 GeV energy band, corresponding to an isotropic equivalent energy of 2.4×10^{53} erg $< E_{iso} < 3.6 \times 10^{53}$ erg (0.1–100 GeV rest frame).

In order to put GRB 221009A in the context of other LAT-detected GRBs we compared some of its characteristics with those in [9]. We found that it is by far the longest GRB ever detected by LAT, with a total duration of $\sim 2 \times 10^5$, corresponding to over two days. Moreover, GRB 221009A represents an outlier in terms of flux lightcurve, showing an extremely high pulse lasting several hundred seconds during the prompt phase, and a late time emission being on the highest end of the GRB distribution. On the other hand, if we take into account its distance, its luminosity is comparable with other bright LAT-detected GRBs. Given its proximity, GRB 221009A is surprisingly more energetic than other GRBs at a similar redshift, and it is as energetic as other energetic GRBs at redshift > 2. Considering the difference in comoving volume confined within $z = 0.151$ and $z > 2$, this demonstrates unequivocally that GRB 221009A is an extremely rare event.

Regarding the burst high-energy photons, we note an interesting coincidence: for the previous record holder, GRB 130427A, the highest energy event was a 94 GeV photon arriving at 243 s after the trigger, almost exactly the same numbers as for the 99 GeV event from GRB 221009A.
With respect to the population of LAT GRBs, the 400 GeV photon clearly stands out. We performed several cross checks and conclude that the chance probability that an event above 100 GeV is detected within 33 ks after the GBM trigger and in spatial coincidence with the burst is slightly below 4σ. Thus we cannot firmly exclude that the photon is a background event. Given the proximity to the Galactic plane and the absence of nearby point sources, it could be likely associated with the diffuse emission from the Milky Way or from the unresolved population of blazars that constitute the majority of the extragalactic gamma-ray background. On the other hand, if we assume that the high-energy event is indeed associated with the GRB, the probability that the event is generated from the high-energy extrapolation of the low-energy part of the spectrum is relatively low ($\approx 5\sigma$), suggesting that the event is either not related to the GRB, or has been produced by an unconventional emission mechanism.

Acknowledgments

The *Fermi*-LAT Collaboration acknowledges support for LAT development, operation and data analysis from NASA and DOE (United States), CEA/Irfu and IN2P3/CNRS (France), ASI and INFN (Italy), MEXT, KEK, and JAXA (Japan), and the K.A. Wallenberg Foundation, the Swedish Research Council and the National Space Board (Sweden). Science analysis support in the operations phase from INAF (Italy) and CNES (France) is also gratefully acknowledged. This work is performed in part under DOE Contract DE-AC02-76SF00515.

References

[1] Castro-Tirado A. J., et al., GRB 221009A: 10.4 m GTC spectroscopic redshift confirmation, 2022, *GRB Coordinates Network* **32686**

[2] Lesage S., et al., GRB 221009A: Fermi GBM observation, 2022, *GRB Coordinates Network* **32642**

[3] Dichiara S., et al., Swift J1913.1+1946 a new bright hard X-ray and optical transient", 2022, *GRB Coordinates Network* **32632**

[4] Atwood W., et al., Pass 8: Toward the Full Realization of the Fermi-LAT Scientific Potential, 2013, *ArXiv e-prints* **1303.3514**

[5] Vianello G., et al., The Multi-Mission Maximum Likelihood framework (3ML), 2015, *ArXiv e-prints* **1507.08343**

[6] Atri P., et al., High-precision position of the compact radio counterpart to GRB221009A, 2022, *GRB Coordinates Network* **32907**

[7] Lesage S., et al., Fermi-GBM Discovery of GRB 221009A: An Extraordinarily Bright GRB from Onset to Afterglow, 2023, *ArXiv e-prints* **2303.14172**

[8] Poolakkil s., et al., The Fermi-GBM Gamma-Ray Burst Spectral Catalog: 10 yr of Data, 2021, *The Astrophysical Journal* **913**

[9] Ajello M., et al., A Decade of Gamma-Ray Bursts Observed by Fermi-LAT: The Second GRB Catalog, 2019, *The Astrophysical Journal* **878**

[10] Xia Z. et al., GRB 221009A: a 397.7 GeV photon observed by Fermi-LAT at 0.4 day after the GBM trigger, 2022, *GRB Coordinates Network* **32748**